Following the Molecular Mechanism of Decarbonylation of Unsaturated Cyclic Ketones Using Bonding Evolution Theory Coupled with NCI Analysis

Supplementary material

Zahedi, Ehsan; Shaabani, Samaneh & SHIROUDI, Abolfazl (2017) Following the Molecular Mechanism of Decarbonylation of Unsaturated Cyclic Ketones Using Bonding Evolution Theory Coupled with NCI Analysis. In: JOURNAL OF PHYSICAL CHEMISTRY A, 121(44), p. 8504-8517.

DOI: 10.1021/acs.jpca.7b08503
Handle: http://hdl.handle.net/1942/25156

Supporting Information

Following the Molecular Mechanism of Decarbonylation of Unsaturated Cyclic Ketones Using Bonding Evolution Theory Coupled with NCI Analysis

Ehsan Zahedi[a,†], Samaneh Shaabani[a], Abolfazl Shiroudi[b]

[a] *Physical Chemistry Department, Shahrood Branch, Islamic Azad University, Shahrood, Iran*

[b] *Center of Molecular and Materials Modelling, Hasselt University, Agoralaan, Gebouw D, B-3590 Diepenbeek, Belgium*

Figure S1. Color−filled maps of the ELF plotted around the C_1, C_6, and C_7 atoms; and snapshots of the ELF localization domains (η=0.8–0.81; Color code: black for core basins, gray for protonated disynaptic basins, blue for disynaptic basins, red for monosynaptic basins of O atom, and green for monosynaptic basins of C atom) for reactant and turning points separating the SSDs along the decarbonylation of **CHD**.

Figure S2. Color−filled maps of the ELF plotted around the C_1, C_4, and C_5 atoms; and snapshots of the ELF localization domains (η=0.8–0.81; Color code: black for core basins, gray for protonated disynaptic basins, blue for disynaptic basins, red for monosynaptic basins of O atom, and green for monosynaptic basins of C atom) for reactant and turning points separating the SSDs along the decarbonylation of **CPE**.

Figure S3. Color−filled maps of the ELF plotted around the C_1, C_4, and C_7 atoms; and snapshots of the ELF localization domains (η=0.8–0.81; Color code: black for core basins, gray for protonated disynaptic basins, blue for disynaptic basins, red for monosynaptic basins of O atom, and green for monosynaptic basins of C atom) for reactant and turning points separating the SSDs along the decarbonylation of **BCH**.

Figure S4. 2D NCI plots of the RDG, s (**r**), versus the electron density multiplied by the sign of the second Hessian eigenvalue λ_2 ρ (**r**); and 3D NCI plots (isosurfaces) of the RDG, s (**r**), correspond to s = 0.5 a.u. and NCI color scale of $-0.05 < \rho < 0.05$ a.u. using SCF densities for reactant and turning points separating the SSDs along the decarbonylation of **CHD**.

Figure S5. 2D NCI plots of the RDG, s (**r**), versus the electron density multiplied by the sign of the second Hessian eigenvalue λ_2 ρ (**r**); and 3D NCI plots (isosurfaces) of the RDG, s (**r**), correspond to s = 0.5 a.u. and NCI color scale of $-0.05 < \rho < 0.05$ a.u. using SCF densities for reactant and turning points separating the SSDs along the decarbonylation of **CPE**.

Figure S6. 2D NCI plots of the RDG, s (**r**), versus the electron density multiplied by the sign of the second Hessian eigenvalue λ_2 ρ (**r**); and 3D NCI plots (isosurfaces) of the RDG, s (**r**), correspond to s = 0.5 a.u. and NCI color scale of $-0.05 < \rho < 0.05$ a.u. using SCF densities for reactant and turning points separating the SSDs along the decarbonylation of **BCH**.

† Corresponding author. Tel: +98 912 2733755; Fax: +98 23 32344634

E-mail addresses: e_zahedi@iau-shahrood.ac.ir; e_zahedi1357@yahoo.com

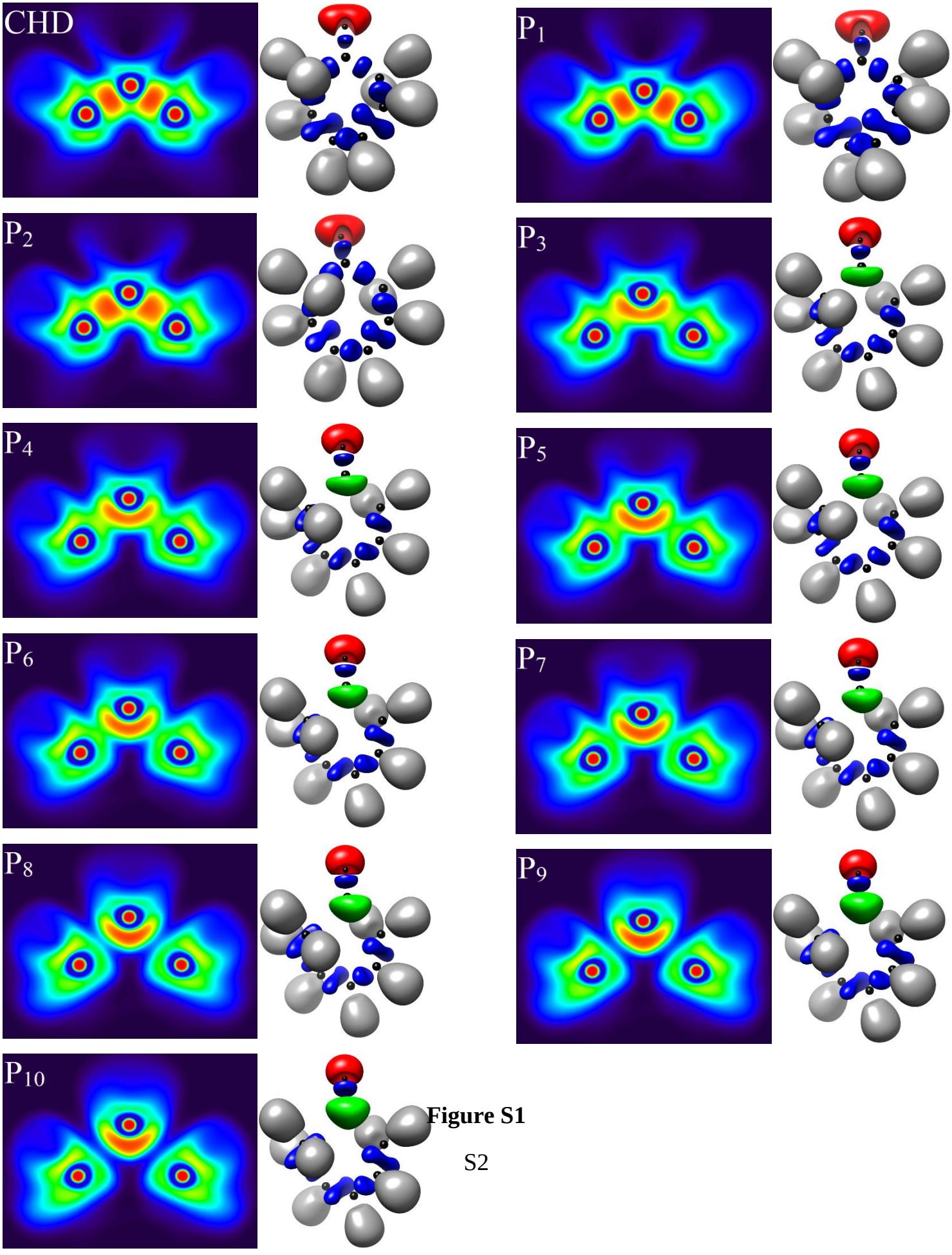

Figure S1

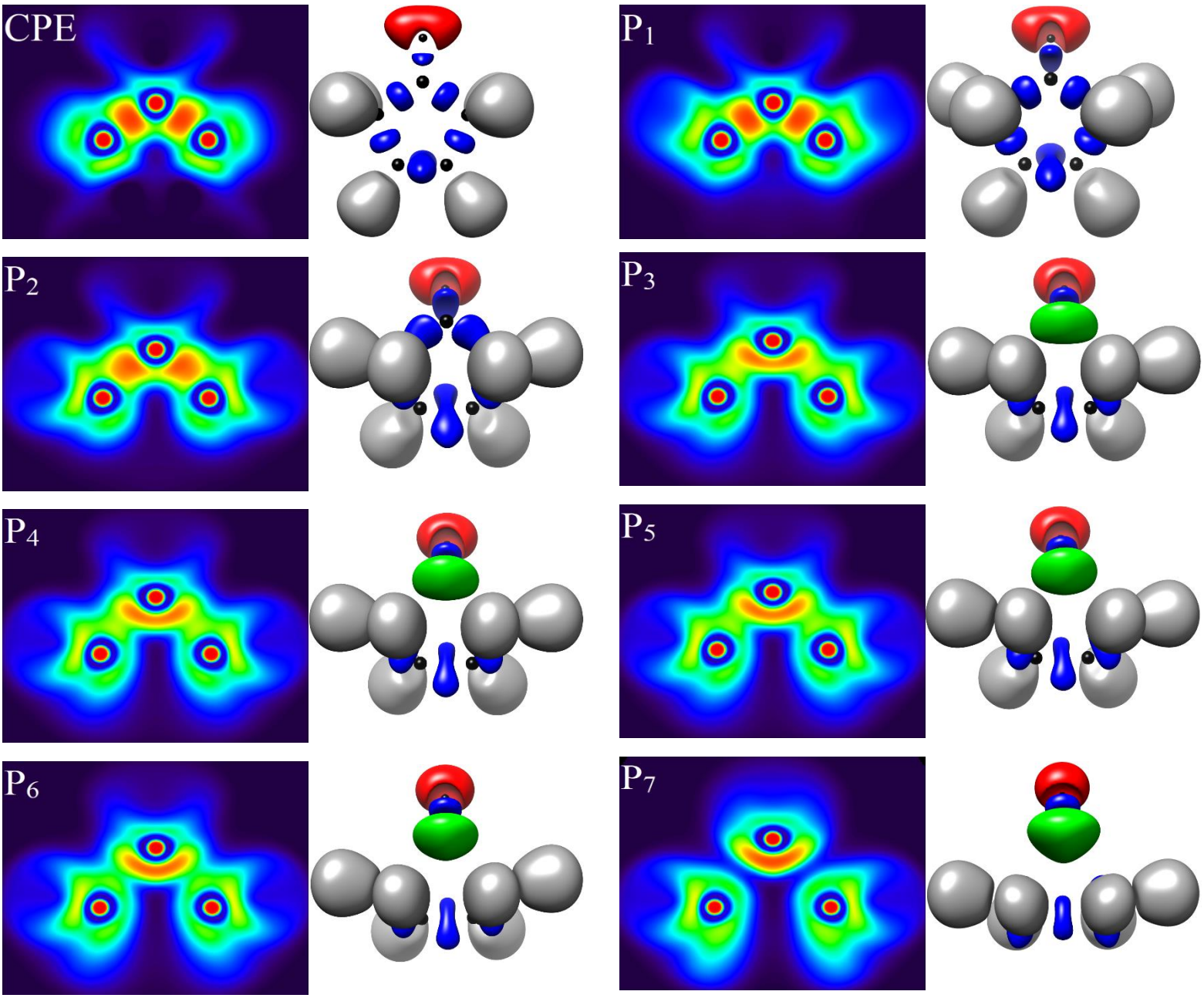

Figure S2

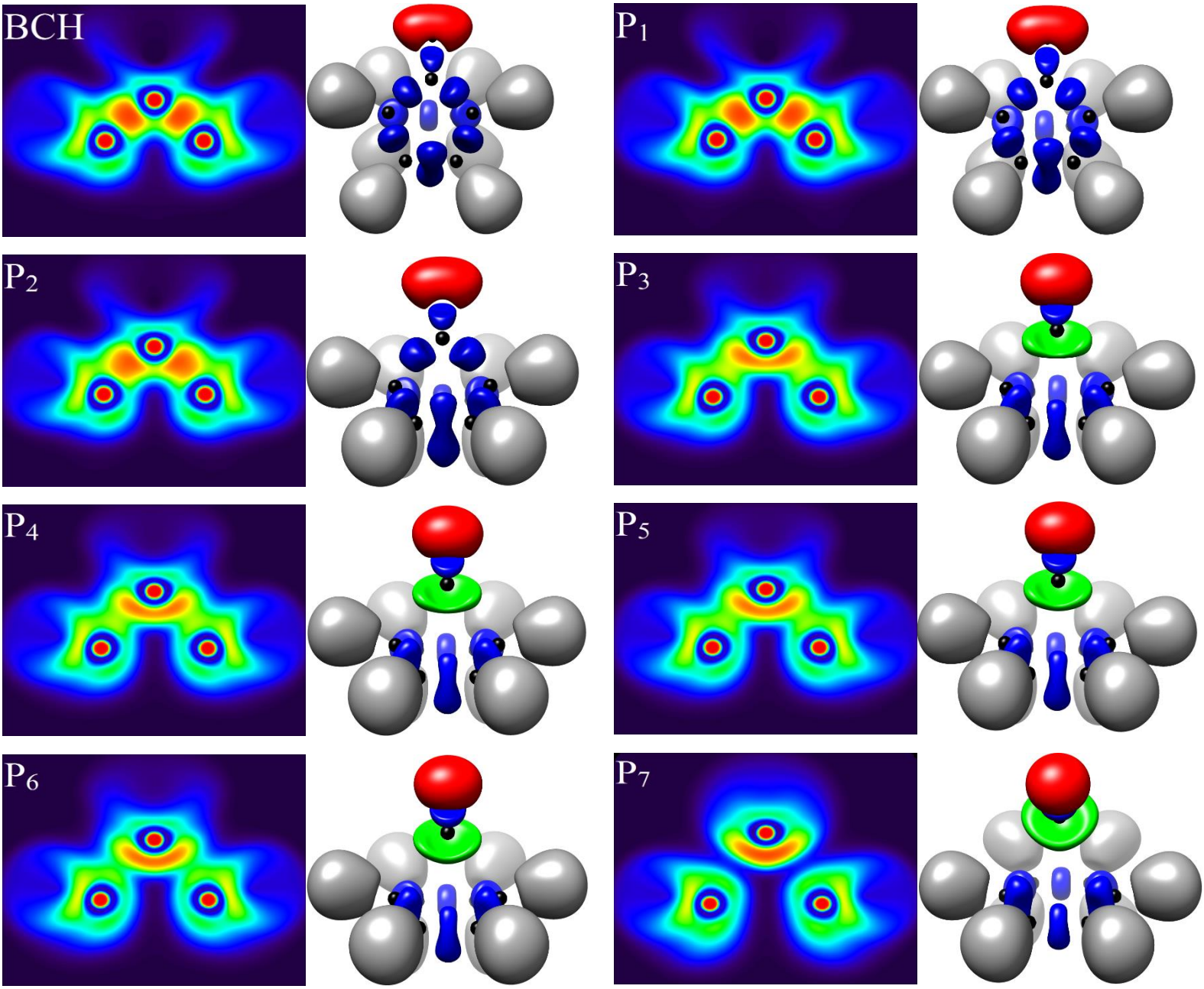

Figure S3

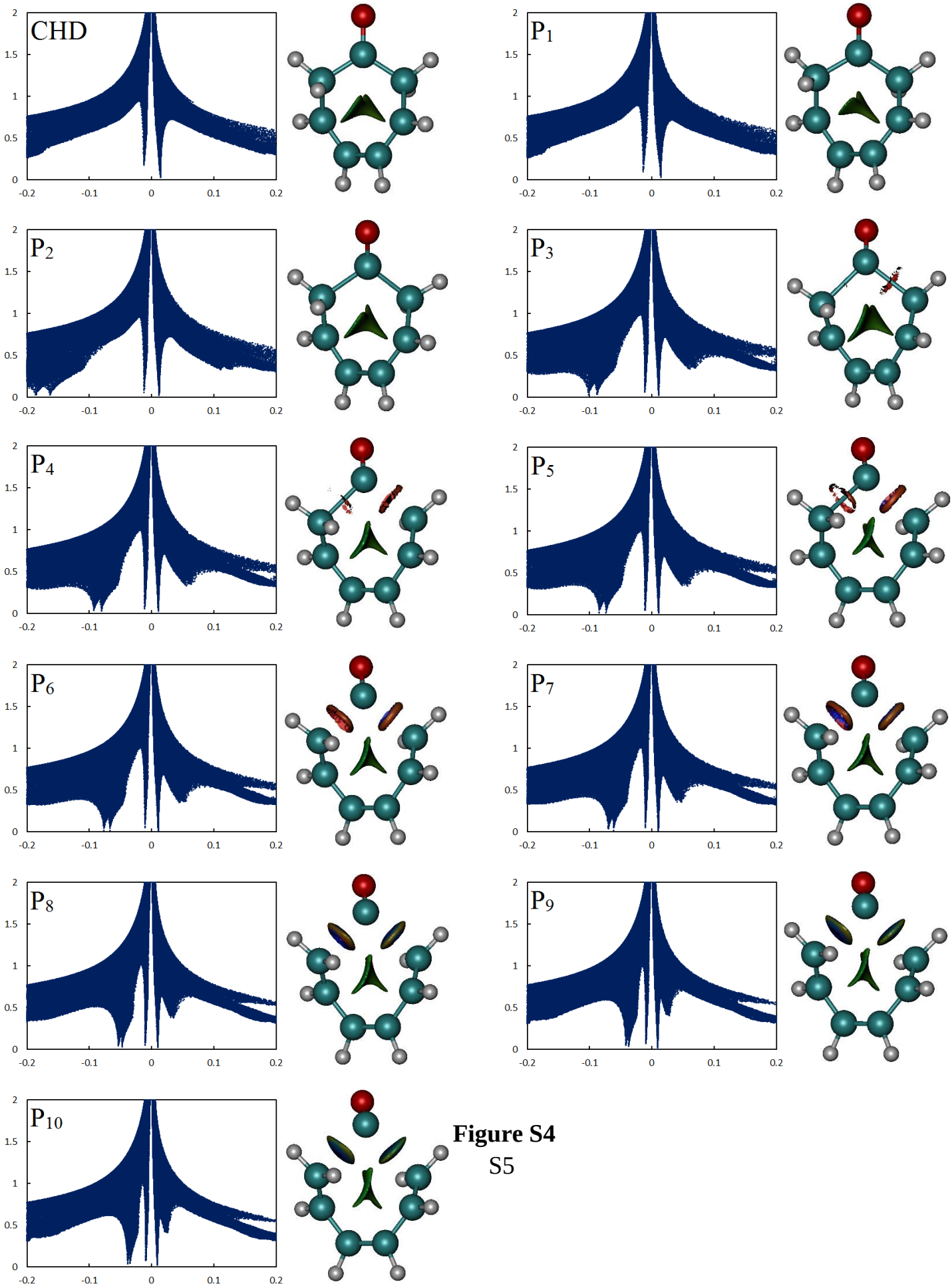

Figure S4

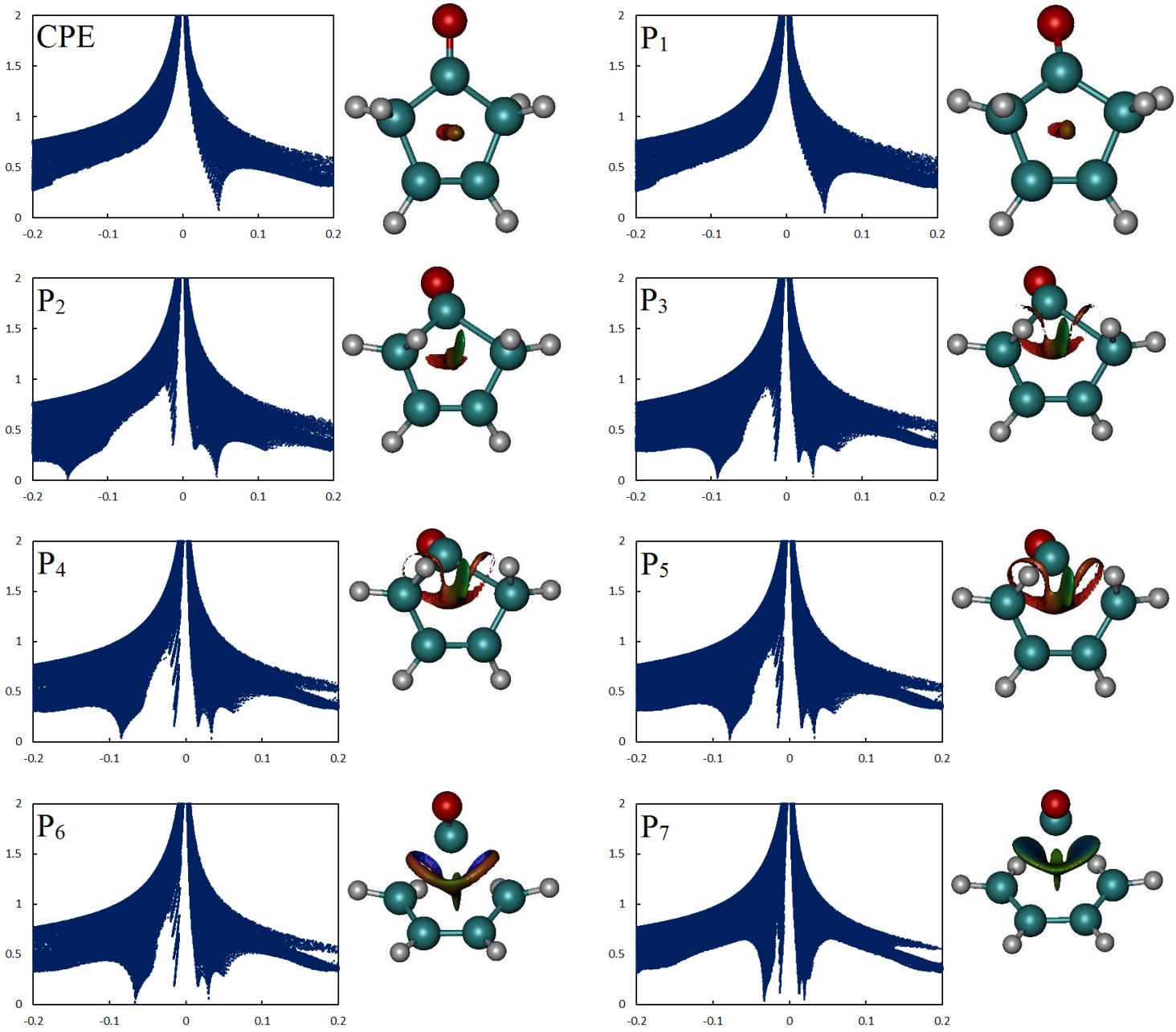

Figure S5

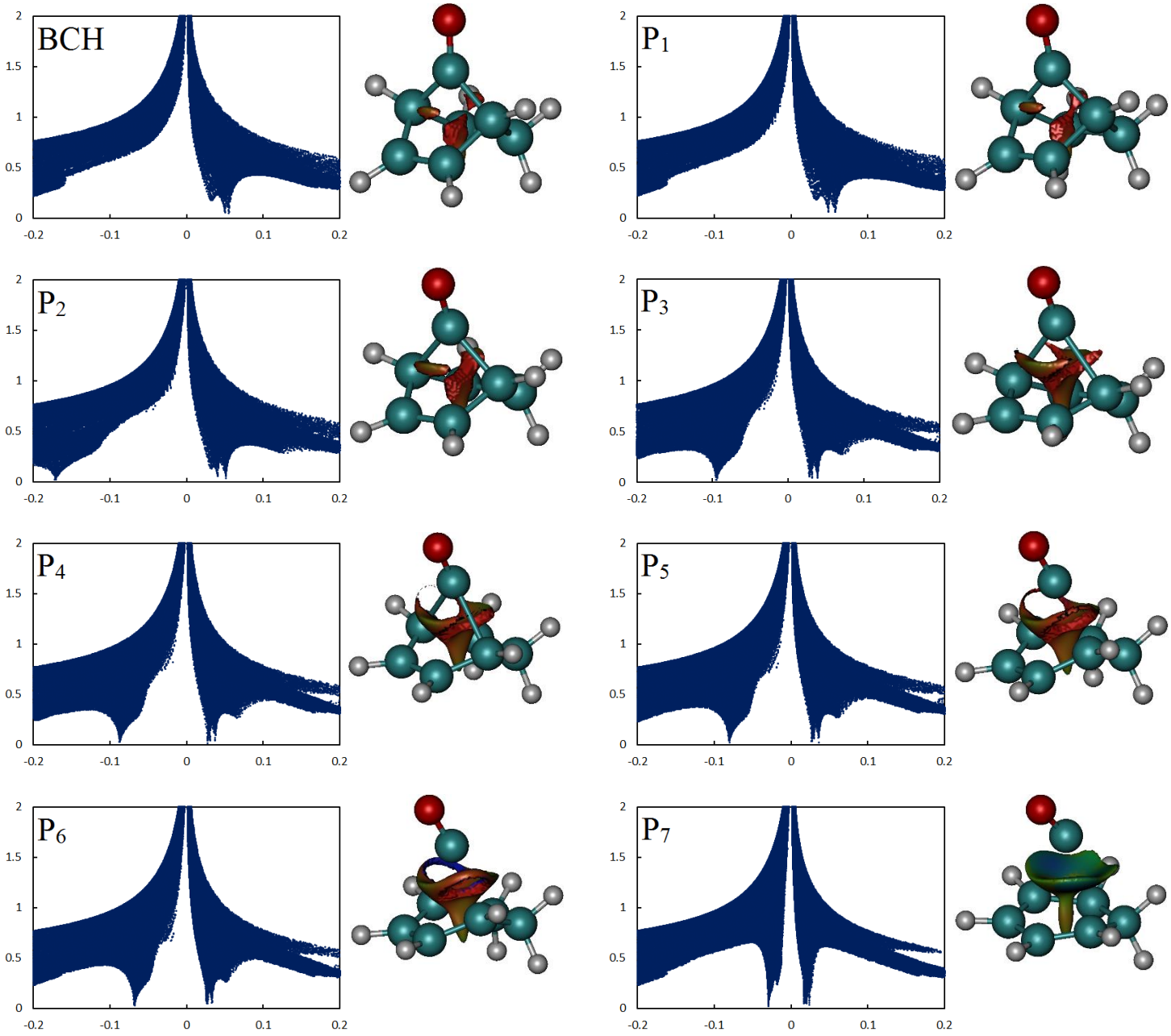

Figure S6